2010 IEEE International Conference on Robotics and Automation
Anchorage Convention District
May 3-8, 2010, Anchorage, Alaska, USA

Control of a Hydraulically-Actuated Quadruped Robot Leg

Michele Focchi, Emanuele Guglielmino, Claudio Semini, Thiago Boaventura, Yousheng Yang and Darwin G. Caldwell

Abstract— **This paper is focussed on the modelling and control of a hydraulically-driven biologically-inspired robotic leg. The study is part of a larger project aiming at the development of an autonomous quadruped robot (hyQ) for outdoor operations. The leg has two hydraulically-actuated degrees of freedom (DOF), the hip and knee joints. The actuation system is composed of proportional valves and asymmetric cylinders. After a brief description of the prototype leg, the paper shows the development of a comprehensive model of the leg where critical parameters have been experimentally identified. Subsequently the leg control design is presented. The core of this work is the experimental assessment of the pros and cons of single-input single-output (SISO) vs. multiple-input multiple-output (MIMO) and linear vs. nonlinear control algorithms in this application (the leg is a coupled multivariable system driven by nonlinear actuators). The control schemes developed are a conventional PID (linear SISO), a Linear Quadratic Regulator (LQR) controller (linear MIMO) and a Feedback Linearisation (FL) controller (nonlinear MIMO). LQR performs well at low frequency but its behaviour worsens at higher frequencies. FL produces the fastest response in simulation, but when implemented is sensitive to parameters uncertainty and needs to be properly modified to achieve equally good performance also in the practical implementation.**

I. Introduction

The development of power autonomous robots is a topic of increasing interest and this work considers this need within the scope of a larger project targeting the development of a hydraulically-actuated autonomous quadruped robot named HyQ [1] whose size is similar to that of a small horse.

The main aim of the HyQ project is to develop a robot able to perform dynamic tasks such as walking, trotting running and jumping, and operate outdoors with an acceptable degree of autonomy. It can find applications in a variety of tasks such as carrying heavy loads, demining, rescuing people or carrying goods in areas not reachable with wheeled vehicles or other conventional means. Furthermore, it can constitute a platform to study and test the use of fluid power to actuate legged robots, in particular novel hydraulic configurations and high efficiency hydraulic drives. It will also allow to undertake experimental research on quadrupedal locomotion.

A competitive advantage of hydraulic drives is their high power-to-weight ratio and fast dynamic response; furthermore such drives are designed to work reliably in outdoor environments. The quest for compactness, the need to deal with heavy payloads and react quickly to external actions has caused in recent years a renewed interest in hydraulic power to actuate robots. This occurred after fluid power has been disregarded as an actuation means for robots for a number of years, although early robotic systems used to be hydraulically powered, e.g. the GE quadruped robot [2] by Liston and Mosher and Raibert's robots [3], [4].

The reasons why hydraulics has been overlooked for a long time can be explained as follows: this technology has been negatively perceived as dirty (leakage is inherent to hydraulics), dangerous (oil is flammable), bulky (often components in the marketplace are heavy and large-sized, even those for mobile applications), noisy (fluid borne noise generation), difficult (to design and to control) and having low efficiency (as opposed to PWM electric drives).

However fluid power, despite being a mature technology has steadily progressed over recent years, also driven by the need of the automotive industry. As a consequence the overall performance of today's smart hydrotronic systems are generally superior to classical hydraulic servos. This technological trend is offering to roboticists a wealth of potentially appealing actuation devices. It ought to be firstly remarked that if robots are designed for outdoor use the issue of leakage (cleanliness) is less critical and at any rate has improved gradually over the years due to the advances in sealing technology. A number of novel high efficiency fluid modulation schemes is currently being investigated, namely variable displacement pump systems [9], digital hydraulics [10] and hydraulic switching converters, that can be seen as the fluidic equivalent of electric DC-DC converters. These latter are being studied for application on the HyQ robot [11].

The rediscovery of fluid power can seen by some recent robotic platforms such as the hopping robot Kenken [12], the work by Hyon and Cheng (2007) at ATR Computational Neuroscience Laboratories in Tokio [13], by Bentivegna and Atkeson (2007) at Carnegie Mellon University [14] on humanoid robots and the BigDog project, by Boston Dynamics [15] (2008). All these projects show significant potential for fluid power as a means to actuate robots.

The control of hydraulic systems is not trivial because their nonlinear behaviour can make their design and tuning a complicated task. The proportional-integral-derivative (PID) controller is extensively used in hydraulics ([16], [17]) as is in many other areas of engineering [18]. However, if specifications are more stringent there is scope to evaluate different control strategies such as adaptive [19] or robust control strategies [20]. From an implementation viewpoint it should be noted that in real systems fluid borne noise (e.g.,

Michele Focchi, Emanuele Guglielmino, Claudio Semini, Thiago Boaventura, Yousheng Yang and Darwin G. Caldwell are with the Italian Institute of Technology, Via Morego 30, 16163 Genoa, Italy. {Michele.Focchi, Emanuele.Guglielmino, Claudio.Semini, Yousheng.Yang, Thiago.Boaventuracunha, Darwin.Caldwell}@iit.it.

gear pump-induced flow and pressure ripple) often deteriorates sophisticated controllers performance [22].

Robotic joints are typically position- or force-controlled. In this application the leg is fixed to a table in its swing phase, so position control is more appropriate. In case of ground contact, particularly on uneven terrains force control or a synergetic combination of position and force control could be advantageous.

Three control schemes are presented. A PID controller (SISO linear), a Linear Quadratic Regulator (LQR) (linear MIMO) and a Feedback Linearisation (FL) scheme (nonlinear MIMO). Each has been simulated and implemented on the leg and experimentally assessed.

In this paper: section II briefly describes the leg prototype; section III introduces the system modelling and parameters identification; section IV describes the controller design and section V is concerned with the simulation and the experimental study. Finally, section VI addresses the conclusions and comments on further developments.

II. Leg prototype

Quadruped animals gait is generally stable and robust in most terrains where animals move. The robotic leg design should aim at reaching an acceptable level of robustness.

The HyQ leg prototype is built in aluminium alloy and stainless steel and is composed of two limb segments: the femur and the tibia, each of length of 0.3 m (Fig. 1). The leg mass and inertia were reduced as much as possible to reduce the power consumption. The prototype leg has three DOF, two hydraulically-actuated DOF and a passive one (all in the sagittal plane). The hydraulic cylinders create triangular configurations between the hip and the two leg segments.

The range of motion of the two DOF in the sagittal plane is inspired by the biomechanics of a Labrador Retriever [1]. Both hip/shoulder and knee/elbow flexion/extension joints can rotate 120°. To increase the gait efficiency through appropriate potential energy storage and release, some passive leg compliance was introduced by designing a foot in visco-elastic rubber linked with a spring.

Experimental tests on the leg has been constrained to a table (as shown in the video).

III. Leg actuation design and modelling

The design of the leg hydraulic actuation, being part of a more complex system, requires a systems engineering approach that caters for all static and dynamic requirements. The HyQ robot hydraulic actuation should be a compact, well-engineered system, comprising a pump, its oil tank, control valves, cylinders and all other required equipments (e.g. filter, cooler, tubing, hosing etc).

The core of the leg actuation are two 4-way proportional valves (Wandfluh WDP-F-A03-ACB-S5-G24) driven by an external power pack comprising an AC motor powered positive displacement pump in parallel with a relief valve, an accumulator and a filtering and a cooling unit.

The valves modulate flow in two double-acting unequal area hydraulic cylinders (Hoerbiger LB6-1610-0070-4M), whose motion produces hip and knee rotations. Fig. 1 shows a scheme of the valve-actuator ensemble for each DOF. The valves and cylinders are off-the-shelf components chosen to selected for compactness, low weight, and high force criteria.

A 160 bar supply was chosen to give a reasonable flow consistent with the capability of the components (cylinders, valves, hoses etc).

The hydraulic dynamic specifications are defined based on the trajectories (gait patterns) for the different locomotion modes. These form periodic waveforms with a first harmonic from 1 Hz (walking) up to 2-3 Hz (running), hence proportional valves (with overlap) were chosen. These valves have a bandwidth of around 30-40 Hz as opposed to the 200Hz possible in more costly servovalves. Dynamic response mainly depends on volumes and on the oil bulk modulus (the reciprocal of oil compressibility). Volumes were reduced as much as feasible and the chosen pressure level was sufficiently high to reduce the risk of free air formation which would adversely affect oil stiffness [23-24].

The nonlinear leg dynamics and the kinematic relations that link piston and joint motion (Fig. 2) are described in [25]. The electro-hydraulic servo-system is modelled using force and continuity equations. It is assumed that the systems uses a linearly compressible fluid and a varying capacity in both cylinder chambers [6]. Bernoulli's equation describes the flow through valve metering edges, a 2nd order spring-mass-damper system dynamics accounts for the valve spool motion and a 1st order lag for the valve solenoid. The pump, relief valve and the accumulator are treated as a constant pressure source p_S and the return line is connected to the tank at atmospheric pressure p_T. Oil temperature was assumed to be constant in the model as an air cooler is present in the oil delivery line keeping oil temperature at around 45 °C.

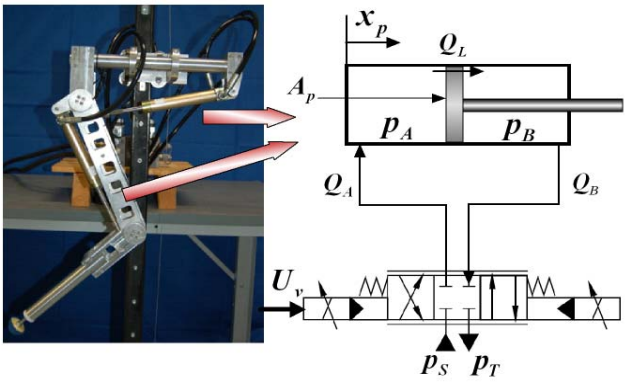

Fig. 1. Picture of the leg (left) and schematic of the leg hydraulic drive for each DOF (right).

If the continuity equation is applied to an asymmetric cylinder, the pressure dynamics in the cylinder chambers is:

$$\dot{p}_A = \frac{\beta_{eff}}{V_A}(Q_A + Q_L - A_p\dot{x}_p) \quad (1)$$

$$\dot{p}_B = \frac{\beta_{eff}}{V_B}(-Q_B - Q_L + \alpha A_p\dot{x}_p) \quad (2)$$

where V_A and V_B are the volumes of the chambers (both variable) including the connecting hoses. Q_A and Q_B are the metering flows to/from the cylinder, A_p is the piston area and

α is the piston/piston ring area ratio. Q_L is the internal laminar leakage between the two chambers which is proportional to the pressure difference between them; β_{eff} is the bulk modulus, the physical property of the fluid that governs its stiffness and mainly affects the servo dynamic behaviour. It depends on the oil compressibility, the air present in the oil and the hoses and pipes elasticity.

For control purpose, a linearised model has been developed and a state space model has been subsequently obtained for the overall (leg and actuation) system:

$$\begin{cases} \dot{X}_o = A_o X_o + B_o U_o \\ Y_o = C_o X_o \end{cases} \quad (3)$$

where the state vector X_o includes the joint angular positions and angular velocities, position and velocity of both cylinder rods, solenoid currents of both valves and hydraulic forces produced by the cylinders. As some hydraulic dynamics are typically fast relative to leg dynamics and not all states are measurable (in particular valve spool positions and velocities), an experimental assessment was carried out to evaluate if these dynamics could be neglected and a reduced state space model developed [21]. This is important from a control perspective as, depending on the control algorithm implemented, state observers (e.g. a Luenberger observer) could be introduced making the design more complex with non-trivial performance and stability issues, as the use of an observer affects the attractive stability margin characteristics of some algorithms [16].

The assessment was initially performed on the valve alone, with the dynamic performance assessed via the frequency response. Fig. 3 shows the magnitude Bode plot of the output pressure v solenoid input voltage transfer function which has a cut-off frequency of approx.35 Hz. The solenoid dynamics (not presented here) is even faster (typically 100 Hz).

Being a magnitude faster than the reference trajectories the states corresponding to the dynamics of both valves' spools were neglected (solenoid currents and spool positions - velocities) reducing the dynamics from 12th to 6th order.

Since it is not easy nor accurate to estimate hydraulic system parameters using theoretical considerations, an experimental approach was used. A second customised test bench for valve and cylinder parameters measurement has been set up to identify the most significant parameters to be used in the nonlinear and linearised model, such as the flow gain, the valve dead band asymmetry (i.e. different amount of overlap in the positive or negative spool directions, often present in valves due to manufacturing tolerances). The latter is important for a more precise compensation of this nonlinearity (which majorly penalises tracking performance in position control loops) in the controller by using an inverse non-linearity. The cylinder friction force was measured as well. Valve flow gain was determined applying a sinusoidal position reference and obtaining flow as a function of cylinder velocity (measured with a linear potentiometer). Valve dead band asymmetry was assessed measuring piston displacement (in both directions) and valve input voltage. As portrayed in Fig. 4 an asymmetry of 10% is present.

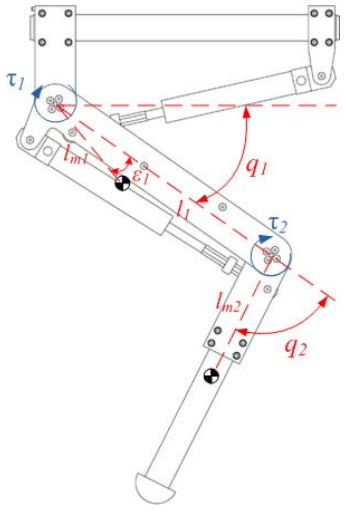

Fig. 2. Geometry of the leg.

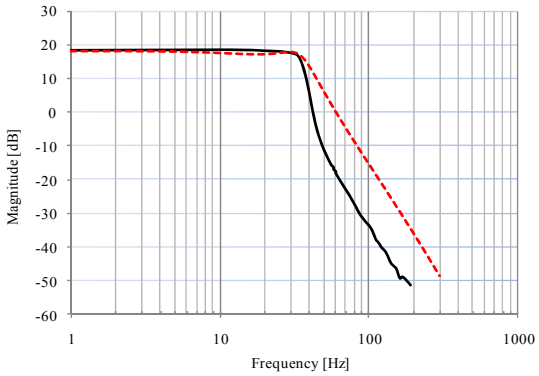

Fig. 3. Valve pressure-to-voltage magnitude Bode diagram: experiments (solid) and simulation (dashed).

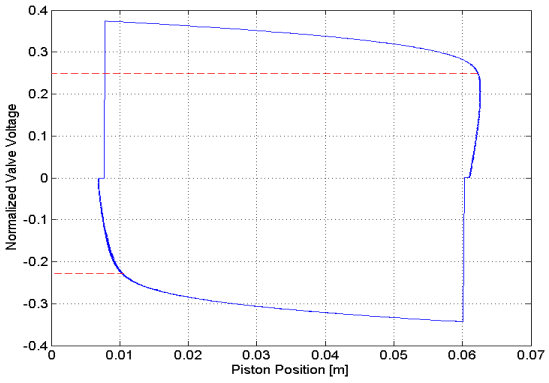

Fig. 4. Valve dead band asymmetry estimation

Friction force in the cylinder was identified by calculating the hydraulic force from chamber pressure measurements at known speeds and inferring the friction force from the force balance equation. Cylinder friction is due to the sliding of the seal against the metal chamber and the oil leakage past the chambers and is tyically Stribeck-type [5]. A Stribeck friction model was hence implemented with a static, a Coulomb and a viscous term, based on the experimental data.

IV. CONTROLLER DESIGN

Leg (and body) motion obeys a set of dynamic laws which must be properly understood and modelled to design high performance closed-loop controllers. Firstly a PID position controller was implemented feeding back joint angular displacements. PID was used to benchmark more sophisticated control schemes, namely LQR and FL.

A force control loop was not implemented at this stage as the leg motion was in air, however, depending on the forms of ground impact it is envisaged that force control may be required in the future. If the impact is short relative to the phase in air (e.g. in running), hybrid position/force algorithms might be a better solution.

A. PID Controller

The PID controller design specifications for the hip and knee were defined based on the step response as follows: rise time (80%) of 0.3 s, settling time (5%) of 0.5 s and maximum overshoot of 10%. The tuned values are shown in Table I:

TABLE I
PID GAINS FOR HIP AND KNEE

Description	Hip	Knee
Proportional gain	0.2	0.16
Integral gain	0.1	0.08
Derivative gain	0.001	0.0016

B. LQR Controller

The second controller developed was an LQR scheme. This is a MIMO controller which seeks to establish a relationship between the energy of the state variables and the control signals [7]. This is achieved by minimising the following cost function:

$$J = min \int_0^\infty [X_o(t)' Q_0 X_o(t) + U_o(t)' R_0 U_o(t)]\, dt \qquad (4)$$

where $X_o(t)$ is the overall linear state vector, $U_o(t)$ is the overall control action, Q_0 the state weighting matrix and R_0 the control weighting matrix. The control law, which minimises the function (4) is of the form:

$$u(t) = -K_{LQR} X_o(t) \qquad (5)$$

with

$$K_{LQR} = {R_0}^{-1} B_o' P \qquad (6)$$

where K_{LQR} is the feedback state gain matrix and P is the (positive semidefinite) solution of the Riccati equation.

The LQR algorithm does not theoretically require tuning if the system is perfectly identified, however its main weakness is that there is no straightforward way of incorporating it into the design of classical system specifications such as rise time, overshoot, settling time, etc. It is necessary to specify the weighting matrices and compare the results with the design goals. In a linearised framework LQR will move the system poles (which are the eigenvalues of the $A_o - B_o K_{LQR}$ matrix) accordingly. Furthermore in this application, in order to have a zero steady-state tracking error two further integrators (one for each joint) have been added in the control loop as depicted in Fig. 5. This results in two additional state variables and hence in an 8th order system.

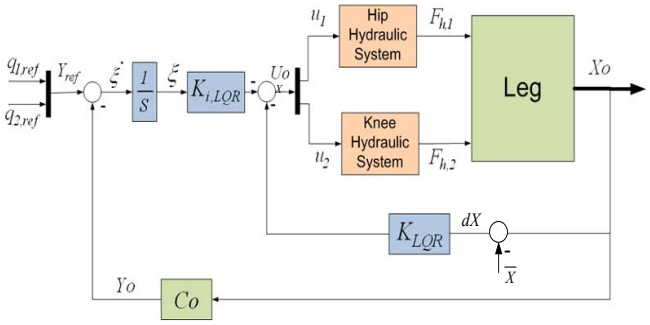

Fig. 5. Closed-loop block diagram of the LQR controller with integrators.

K_{LQR} can be partitioned as follows:

$$K_{LQR} = [K_{s,LQR} \quad K_{i,LQR}] \qquad (7)$$

where $K_{s,LQR}$ is the state gains matrix and $K_{i,LQR}$ is the integrator gains matrix. The simulator tuned values are:

$$K_{s,LQR} = 10^{-3} \begin{bmatrix} 0 & 0 & 436.1 & 7 & 0.5 & 0.1 \\ 0 & 0 & -7 & -439 & -0.1 & -0.1 \end{bmatrix} \qquad (8)$$

$$K_{i,LQR} = \begin{bmatrix} -4.1 & 0.001 \\ -0.001 & 4.18 \end{bmatrix}$$

A sensitivity analysis of the above matrices showed that only 4 entries of the above matrices influence significantly the response.

C. FL Controller

Feedback linearisation aims to convert the nonlinear system dynamics into a (fully or partly) linear one, so that linear control techniques can be applied [8]. The system is coupled and nonlinear, hence it is worth investigating if the use of this nonlinear MIMO control scheme results in an improved response. The approach of the input-output feedback linearisation is to obtain a direct relationship between system output and input, and then to design a control law that cancels the nonlinearities by a feed-forward input which produces a phase advance (predictive behaviour). To obtain this direct relationship the outputs are differentiated repeatedly until the inputs appear in the equations.

Here the system has two outputs (joint angular positions) and two inputs (valve voltages). It is necessary to invert the nonlinearities due to the flow-pressure equations, the hydraulic force dynamics, the lever arm kinematics and the leg dynamics. Valve spool dynamics was neglected since it is faster than leg dynamics; valve overlap can be compensated algebraically with the corresponding inverse nonlinearity, as it is a static nonlinearity.

The leg dynamics are expressed in matrix form as:

$$\ddot{q} = B^{-1}(q)\tau - B^{-1}C(q,\dot{q}) - B^{-1}G(q) \qquad (9)$$

where B, C and G are the inertia, Coriolis and gravity matrices, and q and τ the joint angles and torque vectors respectively. The equation should be differentiated to obtain the derivative of the torque. Since two nonlinear relationships are present (torque vs. hydraulic force due to the lever arm kinematics and force derivative vs. valve voltage) it is possible to obtain a direct relationship between valve voltage and joint angular acceleration and hence position. If torque signs are as in Fig. 2 the following equation can be written:

$$\begin{bmatrix}\dot{\tau}_1\\ \dot{\tau}_2\end{bmatrix}=\begin{bmatrix}\dot{L}_1 & 0\\ 0 & -\dot{L}_2\end{bmatrix}\begin{bmatrix}F_{R1}\\ F_{R2}\end{bmatrix}+\begin{bmatrix}L_1 & 0\\ 0 & -L_2\end{bmatrix}\begin{bmatrix}\dot{F}_{R1}\\ \dot{F}_{R2}\end{bmatrix} \quad (10)$$

where L_1 and L_2 are the joint lever arms, and F_{R1} and F_{R2} the hydraulic forces.

However the derivative of the hydraulic force is also related to the valve voltage U_V through the pressure dynamics and the valve equation:

$$\dot{F}_R = f_F(x) + g_F(x)U_V \quad (11)$$

where $f_F(x)$ contains the effects of leakage, friction and varying capacity of the cylinder chambers and $g_F(x)$ the flow-pressure nonlinearity (an analogous relationship can be obtained for the torque). By differentiating (9) performing some algebraic manipulations yields:

$$\ddot{q} = F_q + G_q U_V \quad (12)$$

F_q and G_q are two matrices accounting for the nonlinerities considered. The following control law is now defined:

$$U_V = {G_q}^{-1}(-F_q + V) \quad (13)$$

where V is a linear term. Therefore the nonlinearities present in (12) are now cancelled and a simple linear triple-integrator system relating the output q and the new input V is obtained:

$$\ddot{q} = V \quad (14)$$

The following control law V is chosen:

$$V=\begin{bmatrix}v_1\\ v_2\end{bmatrix}=\begin{bmatrix}\ddot{q}_{10}\\ \ddot{q}_{20}\end{bmatrix}+ \\ +\begin{bmatrix}k_{1a}(\ddot{q}_{10}-\ddot{q}_1)+k_{1d}(\dot{q}_{10}-\dot{q}_1)+k_{1p}(q_{10}-q_1)\\ k_{2a}(\ddot{q}_{20}-\ddot{q}_2)+k_{2d}(\dot{q}_{20}-\dot{q}_2)+k_{2p}(q_{20}-q_2)\end{bmatrix} \quad (15)$$

where q_{i0}, $\dot{q}_{i0}$, $\ddot{q}_{i0}$ and $\dddot{q}_{i0}$ are the joint reference angles and their derivatives respectively; k_{ip}, k_{id} and k_{ia} gains are chosen to make the system asymptotically stable and to match the design requirements.

An integral term (that helps to cancel the steady-state error in response to a step signal) was not added because in our application our reference signal will be always time-varying.

From an implementation viewpoint, since ${G_q}^{-1}$ is strongly time-varying, it was noted in the experimentation that multiplying it by the control law V as in (13), produces oscillations due to a non-ideal cancellation of the nonlinearities. Hence, in the experiments, a modified control law was implemented that generates the feed-forward action ${G_q}^{-1}(-F_q)$ but applies directly the control action V:

$$U_V = {G_q}^{-1}(-F_q) + V \quad (16)$$

The FL in this form is partly cancelling the nonlinearities but from an implementation viewpoint this is more effective. The gains for the theoretical control law (13) and the modified one (16) are listed in Table II. Note that the range between the smallest and the highest modified gains is reduced by five magnitudes increasing the robustness.

TABLE II
FEEBACK LINEARISATION GAINS

	k_{1a}	k_{1d}	k_{1p}	k_{2a}	k_{2d}	k_{2p}
Theoretical	10	$2\cdot10^4$	$7\cdot10^5$	10	10^3	10^7
Modified	0	0.5	19	0	0.02	75

V. SIMULATION AND EXPERIMENTAL RESULTS

A comparison of the performance of the controllers has been carried out. All position control algorithms were implemented feeding back joint angular displacements using high resolution encoders (Avago, AEDA-3300 Series). The control is executed on a PC-104 based platform connected to a Sensoray 526 data acquisition board that generates the PWM signals (voltage control outputs to valve solenoids). Control algorithms were implemented in C++. A digital third order Butterworth low-pass filter with a cut-off frequency of 30 Hz has been introduced to remove noise on pressure, force and encoder position signals. This has introduced a reasonably small delay (compared to the leg dynamics, which are of the order of few Hz). It is important to filter also the encoder signals in order to have the same delay on all feedback signals of the control loop. Numerical derivatives are computed by using a modified version of the previous low-pass filter. A video showing the controlled leg in operation is attached.

The numerical and experimental response of PID, LQR and FL algorithms to a 1 Hz sinusoidal reference signal (on both joints) having 20° amplitude are shown in Fig. 6, 7 and 8 respectively. The amplitude of the reference signals is fairly high because this was a more severe test.

First the plots relative to the hip joint are presented as this is the most critical from a control viewpoint because of the effects of the lower leg and foot masses. The lower leg joint, with a smaller inertia, is easier to control as shown in Fig. 1.

With reference to Fig. 6 and Fig. 7, LQR and PID have comparable performance and experimental results match well with the simulations.

Further experiments at higher frequencies showed that LQR has a larger phase delay than the PID, Fig. 9. This is due to the fact that the LQR is a linear MIMO algorithm which works well if the system behaves sufficiently close to linearity and with full state feedback, but these circumstances are not met in the investigated system.

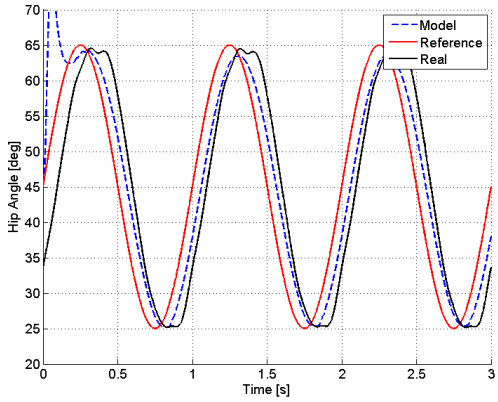

Fig. 6. PID sinusoidal response – model (blue) – real (black).

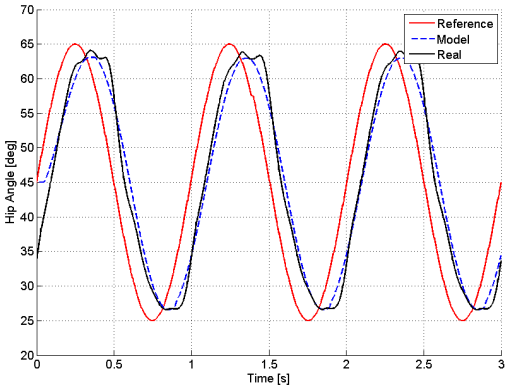

Fig. 7. LQR sinusoidal response – model (blue) – real (black).

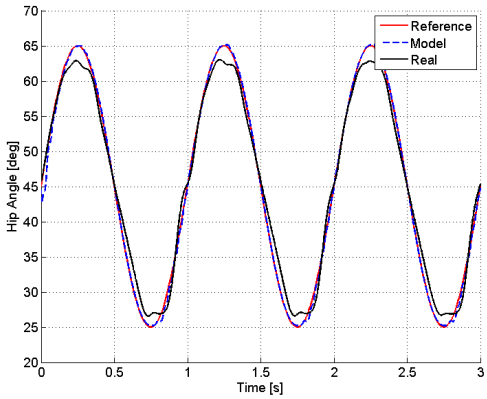

Fig. 8. FL sinusoidal response – model (blue) – real (black).

Fig. 8 shows the performance of FL. In the simulation model the tracking is very good. This was expected because nonlinearities cancel out properly in simulation. FL predictive behaviour can be noticed in its control action plotted in Fig. 10, that is phase-shifted to the left with respect to the PID control action. Fig. 11 shows an experimental comparison of the three algorithms. FL control scheme has the fastest response. This is because it is a model-based control scheme that accounts for the nonlinearities in its design, differently from PID and LQR.

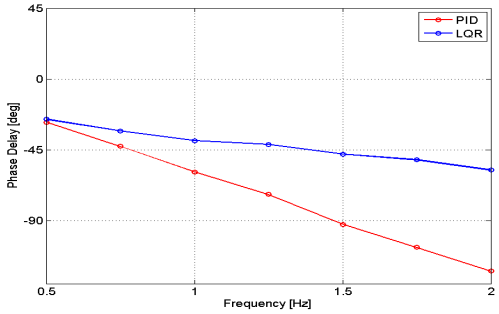

Fig. 9. Reference-angular position phase delay comparison – PID (blue) – LQR (red).

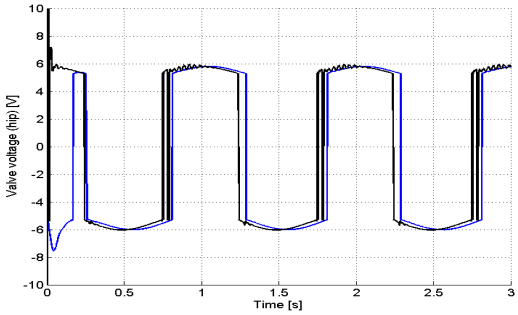

Fig. 10. Simulated control action – PID (blue) – FL (black).

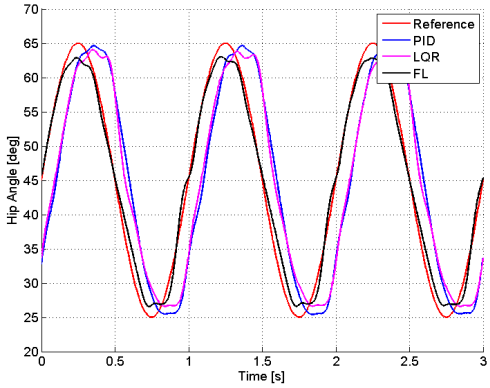

Fig. 11. Hip controllers comparison:PID (blue), LQR (magenta),FL (black).

On the other hand being a model based control it is more sensitive to parameter uncertainty. Modifications were necessary for its practical implementation. Some oscillations are present on the hip trajectory when the whole leg tends to stretch with higher inertia while friction may also have an affect. These oscillations disappear for lower reference inputs. More refined gain tuning and better parameter estimation could help to further enhance FL performance.

As stated before the lower leg joint is easier to control due to smaller mass and inertia. Fig. 12 shows the performance of the three controllers for the knee joint motion.

FL is again the best controller and it can be noted that the tracking is very good also for the almost-stretched leg configuration which is the most critical.

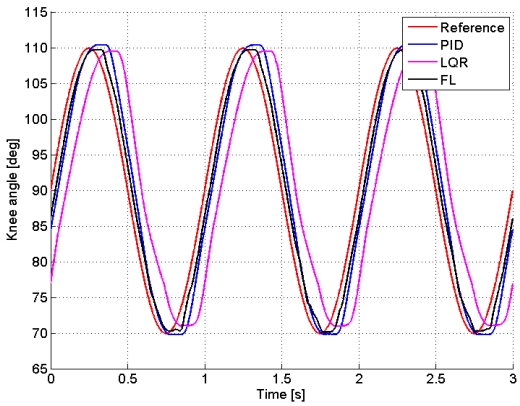

Fig. 12. Knee controllers comparison: PID (blue), LQR (mag), FL (black).

VI. Conclusions and Future Work

A model of a nonlinear hydraulically-actuated two link robot leg driven by nonlinear actuators have been developed and system critical parameters experimentally identified.

A linear SISO controller (PID) has been initially designed and implemented based on a linear model of the system. Subsequently linear MIMO (LQR) and nonlinear MIMO (FL) control schemes have been developed and their performance assessed via simulation and experimentally.

LQR achieves a performance comparable to that of PID both in simulation and experimentally but its performance decreases at higher frequencies. This because LQR is a linear controller designed to work around a steady operating point, whereas the investigated system cannot be approximated as such. The other reason is envisaged to be due to the reduced order state feedback implementation. On the other hand, observers would have added complexity with questionable benefits. Therefore in this instance a linear MIMO approach does not seem to be the best to enhance the performance of a classical linear SISO controller such as a PID.

FL exhibits the fastest response, although some oscillations on the hip joint are present in some configurations. Possible reasons are the higher inertia, together with model uncertainties that lead to a non-ideal cancellation and a poorer position tracking behaviour.

Future work will include the implementation of other types of algorithms (adaptive and robust type), and the implementation of force control and mixed position/force algorithms for ground impact control.

The development of a third actuated DOF for lateral hip motion is being explored concurrently, and if appropriate, comparison will be made with bio-data of a real leg.

Furthermore, the critical issue in autonomous robotics of the trade-off among power consumption, bandwidth and control performance will be addressed in further works by consideration of alternative flow modulation schemes.

References

[1] C. Semini, N. G. Tsagarakis, B. Vanderborght, Y. Yang and D. G. Caldwell, "HyQ – hydraulically actuated quadruped robot: hopping leg prototype," *IEEE/Biorob 2008*, Scottsdale, Arizona, USA.

[2] R. A. Liston and R. S. Mosher, "A versatile walking truck", *Transportation Engineering Conference*, 1968.

[3] M. Raibert, H. J. Brown and M. Chepponis, "Experiments in balance with a 3D one-legged hopping machine," *International Journal of Robotics Research*, vol. 3, no. 2, pp. 75-92, 1984.

[4] M. Raibert, "*Legged robots that balance*," The MIT Press, Cambridge Massachusetts, 1986.

[5] X. Brun, S. Sesmat, S. Scavarda and D. Thomasset, ''*Simulation and Experimental Study of the Partial Equilibrium of an Electropneumatic Positioning System, Cause of the 'Sticking and Restarting Phenomenon'*,'' Proc. 4th Japan Hydraulics and Pneumatics Society Int. Symp. on Fluid Power, Tokyo, Japan, pp. 125–130, 1999.

[6] N. D. Manring, "*Hydraulic control systems*," Wiley, 2005.

[7] B. Friedland, "*Control System design: an introduction to state-space methods*," Dover, 2005.

[8] J. J. E. Slotine and W. Li, "*Applied nonlinear control*," Prentice-Hall, New Jersey, USA, 1991.--

[9] C. Williamson, J. Zimmerman and M. Ivantysynova, "Efficiency study of an excavator hydraulic system based on displacement-controlled actuators," *Proc. Bath Workshop on Power Transmission and Motion Control*, Bath, UK, 2008.

[10] M. Linjama, M. Huova, P. Bostöm, A. Laamanen, L. Siivonen, L. Morel, M. Walden and M. Vilenius, "Design and Implementation of Energy Saving Digital Hydraulic Control System," *The Tenth Scandinavian International Conference on Fluid Power* (*SICFP'07*), Tampere, Finland, 21–23 May 2007.

[11] E. Guglielmino, C. Semini, Y. Yang, D. G. Caldwell, H. Kogler and R. Scheidl, "Energy efficient fluid power in autonomous robotics" accepted at *2009 ASME Dynamic Systems and Control Conference* (*ASME DSCC 09*), Hollywood, LA, CA, October 2009.

[12] S. Hyon, T. Emura and T. Mita, "Dynamics-based control of one-legged hopping robot," *Journal of Systems and Control Engineering*, vol. 217, no. 2, pp. 83-98, April 2003.

[13] S-H. Hyon and G. Cheng, "Simultaneous adaptation to rough terrain and unknown external forces for biped humanoids," *IEEE-RAS 7th International Conference on Humanoid Robots* (*Humanoids 07*), Pittsburgh, PA, USA, 2007.

[14] D. C. Bentivegna, C. G. Atkeson and J-Y Kim, "Compliant control of a hydraulic humanoid joint," *IEEE-RAS 7th International Conference on Humanoid Robots (Humanoids 07)*, Pittsburgh, PA, USA, 2007.

[15] M. Raibert, K. Blankespoor, G. Nelson, R. Playter & the BigDog Team, "BigDog, the rough-terrain quadruped robot," *17th World Congress. The Int. Federation of Automatic Control*, Seoul, Korea, pp. 10822-10825, 2008.

[16] G. Jacazio and G. Bassolini, "A high performance force control system for dynamic loading of fast moving actuators," *Proc. Bath Workshop on Power Transmission and Motion Control*, Bath, UK, 2005.

[17] M. Linjama and T. Virvalo, "Low-order robust controller for flexible hydraulic manipulators," *Proc. Bath Workshop on Power Transmission and Motion Control*, Bath, UK, 2005.

[18] J. C. Hung, "Practical industrial control techniques," *20th International Conference Industrial Electronics, Control and Instrumentation*, (*IECON '94*), pp. 7-14 - Bologna, Italy, 1994.

[19] P. Krus and S. Gunnarson, "Adaptive control of a hydraulic crane using on-line identification," *Proc. Third Scandinavian Conf. on Fluid Power*, Linkoeping, Sweden, 1993.

[20] A. R. Plummer, "Robust electrohydraulic force control," *Proc. of the Institution of Mechanical Engineers Part I - Journal of Systems and Control Engineering*. vol. 221 no. 4, pp. 717-731, 2007.

[21] G. A. Sohl, and J. E. Bobrow, "Experiments and simulations on the nonlinear control of a hydraulic servosystem," *IEEE Trans. on Control Systems Technology*, vol.7, no 2, March 1999.

[22] A. O. Gizatullin and K. A. Edge, "Adaptive control for a multi-axis hydraulic test rig" *Proc of the Institution of Mechanical Engineers Part I - Journal of Systems and Control Engineering*, vol. 221 no. 2, pp. 183-198, 2007.

[23] J. Kajaste, H. Kauranne, A. Ellman and M. Pietola, "Experimental validation of different models for effective bulk modulus of hydraulic fluids," *The Ninth Scandinavian Int. Conf. on Fluid Power*, Linkoeping, Sweden, 2005.

[24] D. McLoy and H. R. Martin, "*Control of fluid power: analysis and design*," Wiley, 1980.

[25] T. B. Cunha, C. Semini, E. Guglielmino, V. J. De Negri and Y. Yang "Gain scheduling control for the hydraulic actuation of the HyQ robot leg," to be presented at *20th International Congress of Mechanical Engineering*, Gramado, RS, Brazil, November 15-20, 2009.